The EMBO Journal Vol. 19 No. 14 pp. 3586–3596, 2000

Munc13-1 acts as a priming factor for large dense-core vesicles in bovine chromaffin cells

Uri Ashery[1], Frederique Varoqueaux[2], Thomas Voets[1], Andrea Betz[2], Pratima Thakur[1], Henriette Koch[2], Erwin Neher[1], Nils Brose[2,3] and Jens Rettig[1,3]

[1]Max-Planck-Institute for Biophysical Chemistry, Department of Membrane Biophysics, Am Fassberg 11, 37077 Göttingen and [2]Max-Planck-Institute for Experimental Medicine, Molecular Neurobiology Group, Hermann-Rein-Strasse 3, 37075 Göttingen, Germany

[3]Corresponding authors
e-mail: brose@em.mpg.de or jrettig@gwdg.de

In chromaffin cells the number of large dense-core vesicles (LDCVs) which can be released by brief, intense stimuli represents only a small fraction of the 'morphologically docked' vesicles at the plasma membrane. Recently, it was shown that Munc13-1 is essential for a post-docking step of synaptic vesicle fusion. To investigate the role of Munc13-1 in LDCV exocytosis, we overexpressed Munc13-1 in chromaffin cells and stimulated secretion by flash photolysis of caged calcium. Both components of the exocytotic burst, which represent the fusion of release-competent vesicles, were increased by a factor of three. The sustained component, which represents vesicle maturation and subsequent fusion, was increased by the same factor. The response to a second flash, however, was greatly reduced, indicating a depletion of release-competent vesicles. Since there was no apparent change in the number of docked vesicles, we conclude that Munc13-1 acts as a priming factor by accelerating the rate constant of vesicle transfer from a pool of docked, but unprimed vesicles to a pool of release-competent, primed vesicles.

Keywords: capacitance measurements/exocytosis/Munc13-1/priming/secretion

Introduction

Secretion of catecholamine from chromaffin cells of the adrenal medulla into the bloodstream plays an important role in cardiovascular and metabolic adaptations of the body during stress situations. Chromaffin cells are derived embryonically from the neural crest, i.e. from the same precursors that give rise to sympathetic neurons, and are regarded as modified sympathetic neurons (Morgan and Burgoyne, 1997). They secrete catecholamine through the fusion of large dense-core vesicles (LDCVs) with the plasma membrane using the same conserved fusion machinery that functions in neurons (Morgan and Burgoyne, 1997). In the last decades, they have been used extensively as a model system to study Ca^{2+}-triggered exocytosis. They offer the unique advantage of applying high time resolution techniques like membrane capacitance measurements and electrochemical detection of catecholamine release for studying exocytosis in the millisecond range (see Neher, 1998 for review). These measurements revealed the existence of different kinetic phases of secretion. A rapid increase in intracellular Ca^{2+} leads to an exocytotic burst followed by a sustained phase of secretion. The burst can be further resolved into two kinetically distinct components, suggesting the presence of two separate release-competent pools of vesicles (Heinemann *et al*., 1994; Voets *et al*., 1999). It recently became possible to overexpress synaptic proteins in chromaffin cells, making them an ideal system to study the role of synaptic proteins in regulated exocytosis (Ashery *et al*., 1999; Duncan *et al*., 1999).

Morphological and fluorescence microscopy studies on chromaffin cells demonstrated that ~450–1000 LDCVs are located near the plasma membrane ('morphologically docked') (Burgoyne, 1991; Parsons *et al*., 1995; Plattner *et al*., 1997; Steyer *et al*., 1997; Oheim *et al*., 1998). In contrast, electrophysiological measurements have demonstrated that, upon stimulation, only a fraction of these vesicles can be rapidly released (Neher and Zucker, 1993; Parsons *et al*., 1995). Thus, the fusion-competent, i.e. primed vesicles (the releasable pools) represent only a small fraction of the 'morphologically docked' vesicles at the plasma membrane. While many of the proteins involved in synaptic transmission and other neurosecretory processes have been identified and cloned (Südhof, 1995), only few of them have been shown to participate in priming. Recently, it was demonstrated that Munc13-1, a presynaptic protein (Betz *et al*., 1998), is essential for a post-docking step in mouse (Augustin *et al*., 1999b), *Caenorhabditis elegans* (Richmond *et al*., 1999) and *Drosophila* (Aravamudan *et al*., 1999), suggesting that Munc13-1 is essential for priming or fusion of synaptic vesicles.

To learn about the role of Munc13-1 in LDCV priming and fusion, we overexpressed Munc13-1 in chromaffin cells with the Semliki Forest virus (SFV) gene expression system (Liljeström and Garoff, 1991). Using flash photolysis of caged calcium as a fast stimulus, we studied the effect of Munc13-1 on the different kinetic components of exocytosis with high time resolution capacitance measurements and electrochemical detection of catecholamine release. We found that Munc13-1 causes a 3-fold increase in the size of the exocytotic burst without changing the time constants for fusion. The sustained component was also increased. Kinetic analysis of the data and simulation by a model suggest that Munc13-1 shifts the vesicle equilibrium from a docked, but unprimed state towards a more mature, fusion-competent state. We conclude that, upon overexpression, Munc13-1 acts as a

priming factor for LDCVs in chromaffin cells. Our results clarify the discrepancy between the number of docked vesicles at the membrane and the number of physiologically releasable vesicles and suggest that priming is a limiting process in adrenal chromaffin cells.

Results

Munc13-1 is expressed at low levels in bovine chromaffin cells

Specific antibodies to Munc13 isoforms (Augustin *et al*., 1999a) and to Munc18 (Hata *et al*., 1993) were used in a comparative western blot analysis of bovine chromaffin cell homogenates, bovine brain synaptosomes and rat brain synaptosomes to determine their respective expression levels. Bovine chromaffin cells express low levels of Munc13-1, Munc13-3 and Munc18, while Munc13-2 is not detectable (Figure 1A). The expression levels of Munc13-1, Munc13-3 and Munc18 in bovine brain synaptosomes were at least five to 10 times higher than those observed in chromaffin cells (Figure 1A and data not shown).

To verify overexpression of full-length Munc13-1–green fluorescent protein (GFP) in infected chromaffin cells, we performed western blot analysis of Munc13-1 expression in infected and uninfected cultures. At the exposure shown in Figure 1B, a monoclonal antibody to Munc13-1 (Betz *et al*., 1998) detected a 220 kDa band in cells infected with SFV–Munc13-1–GFP, but not in uninfected control cells. The band is slightly larger than Munc13-1 from rat brain and corresponds well with the predicted molecular weight of Munc13-1–GFP fusion proteins (223 kDa). Quantitative western blot analysis showed that the ratio of overexpressed Munc13-1–GFP to endogenous Munc13-1 was at least 35:1 (data not shown). Confocal imaging on overexpressing cells revealed that Munc13-1–GFP is evenly distributed throughout the cell (Figure 1C). Since Munc13-1 possesses a phorbol ester-binding domain (C1 domain), it translocated to the plasma

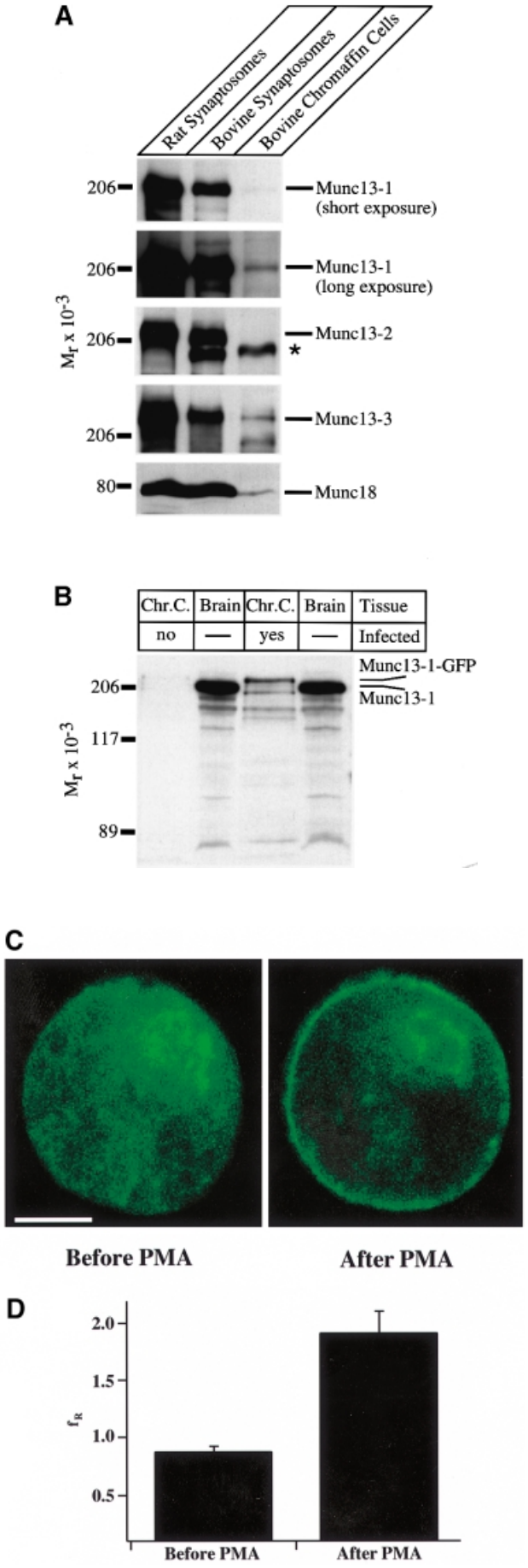

Fig. 1. Endogenous and overexpressed Munc13 isoforms in chromaffin cells. (**A**) Analysis of endogenously expressed Munc13 isoforms in chromaffin cells. Protein samples of indicated origin (20 µg per lane) were separated by SDS–PAGE and blotted onto nitrocellulose. Munc13 isoforms and Munc18 were detected by immunoblotting using specific antibodies. Note that low levels of Munc13-1, Munc13-3 and Munc18 are expressed in bovine chromaffin cells. The asterisk indicates a cross-reactive band of unknown origin present in bovine tissues. (**B**) Overexpression of Munc13-1 in bovine chromaffin cells. Chromaffin cells were infected with SFV–Munc13-1–GFP and harvested 16 h after infection. Protein samples of uninfected (Chr.C, no) and infected (Chr.C, yes) chromaffin cells (20 µg per lane) as well as rat brain synaptosomes (Brain, 20 µg per lane) were separated by SDS–PAGE and blotted on to nitrocelulose. Endogenous Munc13-1 and overexpressed Munc13-1–GFP were detected using a specific antibody directed against the C-terminus of Munc13-1. Note the massive overexpression of Munc13-1–GFP in chromaffin cells that had been infected with SFV–Munc13-1–GFP. (**C**) Distribution of overexpressed Munc13-1–GFP in adrenal chromaffin cells before and after application of 100 nM PMA. Scale bar represents 5 µm. (**D**) Ratio of fluorescence intensities of plasma membrane and cytoplasm before and after PMA application. Before PMA application, Munc13-1–GFP is distributed equally between the plasma membrane and the cytoplasm (f_R = 0.86) while translocation of Munc13-1–GFP to the plasma membrane after PMA application caused an increase of more than 2-fold in the ratio (f_R = 1.89). Error bars represent SEM.

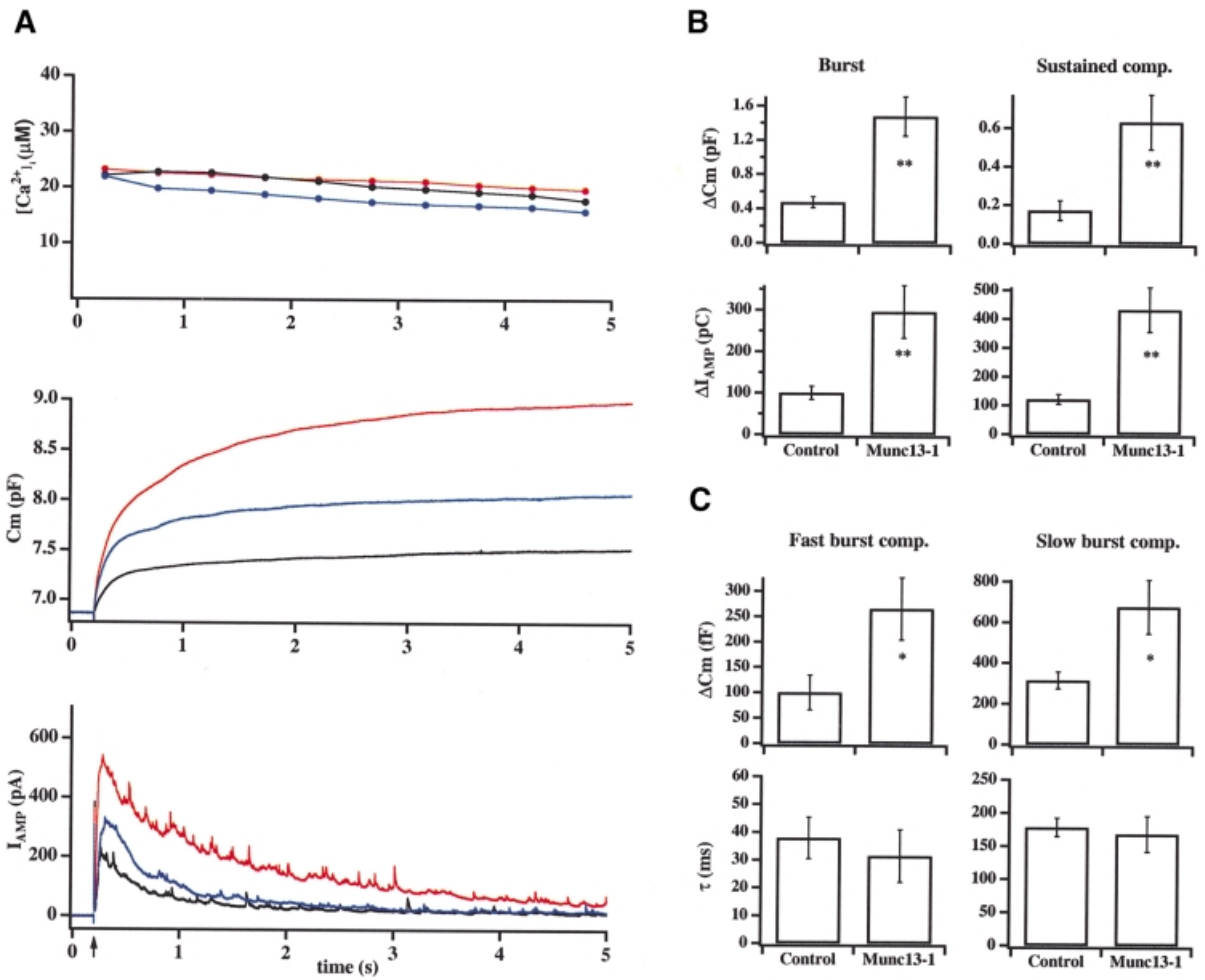

Fig. 2. Munc13-1 overexpression causes a 300% increase in catecholamine secretion in response to flash photolysis of caged calcium. (**A**) Averaged high time resolution recordings of membrane capacitance (Cm; middle trace) and amperometric current (I_{AMP}; lower trace) in response to flash photolysis of caged calcium (indicated by an arrow) from control (black; n = 25), Munc13-1 (red; n = 20) and Munc13-1^{H567K} (blue; n = 15) cells. For all cells, $[Ca^{2+}]_i$ was kept at ~20 μM for 5 s (upper trace). (**B**) The average increase in capacitance during the exocytotic burst (0–1 s) and during the sustained component (1–5 s) were about three times larger in Munc13-1 cells. The integral of the amperometric currents was increased by the same factor in Munc13-1 cells. (**C**) Detailed analysis of the exocytotic burst revealed that the fast (RRP) and the slow burst components (SRP) both increased in Munc13-1 cells (upper panels). In contrast, time constants for secretion were similar for control and Munc13-1 cells (lower panels). Error bars represent SEM. *p <0.02; **p <0.001 (t-test).

membrane upon application of phorbol myristate acetate (PMA) (Figure 1C; Betz *et al*., 1998; Ashery *et al*., 1999). Quantitative analysis of fluorescence intensities revealed that before PMA application, Munc13-1 is evenly distributed between the plasma membrane and the cytoplasm [ratio of fluorescence intensities of plasma membrane and cytoplasm (f_R) = 0.86]. Upon PMA application, the fluorescence ratio changed to 1.89, because more Munc13-1 translocated to the plasma membrane (Figure 1D).

Munc13-1 enhances the exocytotic burst and the sustained component

To determine the role of Munc13-1 in secretion of catecholamine, we performed high time resolution measurements on Munc13-1-overexpressing chromaffin cells. Cells were held in the whole-cell mode to allow both dialysis of the Ca^{2+} cage nitrophenyl–EGTA (NPE; Ellis-Davies and Kaplan, 1994) into the cytoplasm and membrane capacitance measurements. Two to three minutes after establishing the whole-cell configuration, secretion was triggered by flash photolysis of calcium from the NPE while simultaneously measuring membrane capacitance, amperometric currents and intracellular calcium concentration ($[Ca^{2+}]_i$) with high time resolution. In control cells, such step elevation of $[Ca^{2+}]_i$ triggers secretion, which occurs in two phases (Xu *et al*., 1998). A fast exocytotic burst represents the fusion of two populations of release-competent vesicles, the readily and slowly releasable pools (RRP and SRP) (Xu *et al*., 1998; Voets *et al*., 1999), while a second sustained component represents vesicle recruitment/maturation and subsequent fusion (Thomas *et al*., 1993a; Xu *et al*., 1998, 1999a). In cells overexpressing Munc13-1, the average exocytosis, as measured by an increase in membrane capacitance, was markedly larger than that of control cells (Figure 2A, middle trace, red). This was also reflected in a larger amperometric current measured by the carbon fiber, demonstrating that the

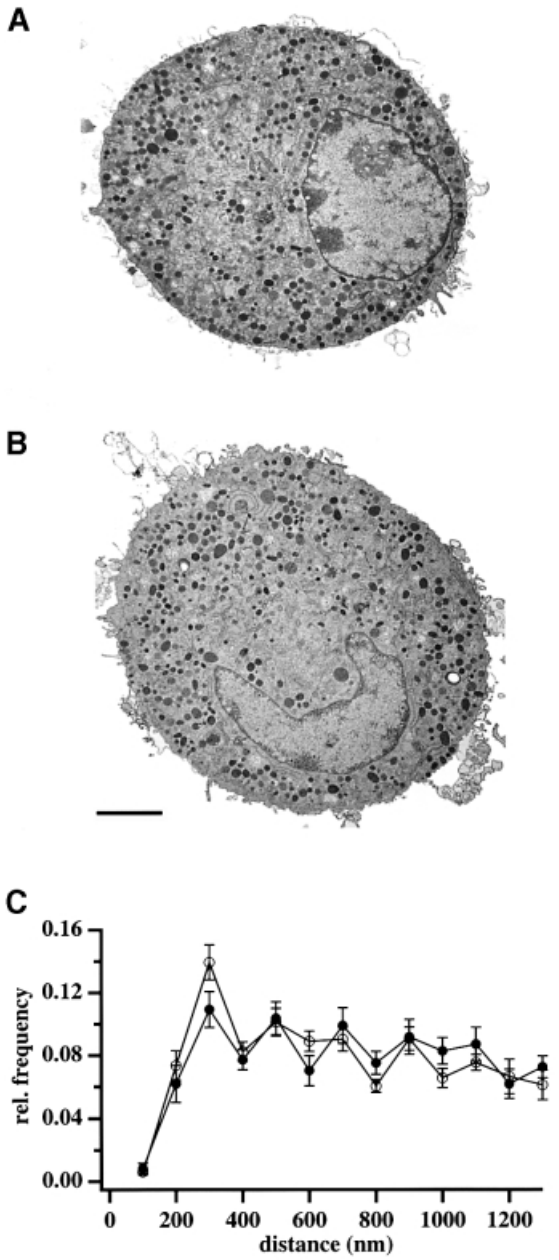

Fig. 3. The number of morphologically docked vesicles is unchanged in Munc13-1 cells. Representative electron micrographs of control (**A**) and Munc13-1-overexpressing (**B**) bovine chromaffin cells. The overall distribution of organelles within a Munc13-1-expressing cell is similar to that of control cell. Dense-core vesicles are distributed homogeneously in the cell interior. (**C**) Quantitative analysis revealed that the fraction of 'morphologically docked' vesicles (≤200 nm from the plasma membrane) and the overall relative frequency (≤1300 nm from the plasma membrane) is similar in control (open circles) and Munc13-1 cells (closed circles). Furthermore, the density of vesicles is similar between control (3.8 ± 0.37 vesicles/μm^2) and Munc13-1 cells (3.7 ± 0.46 vesicles/μm^2). Bar represents 2 μm.

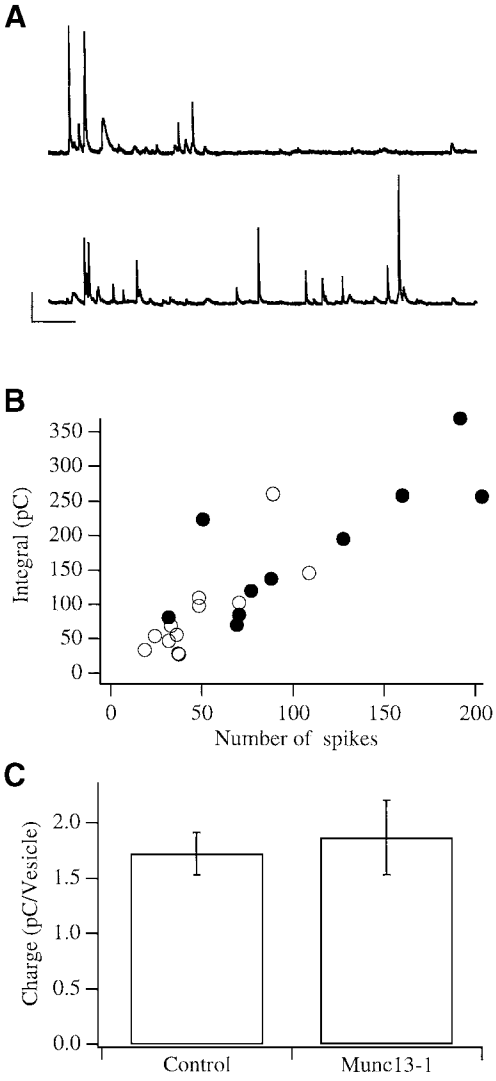

Fig. 4. Munc13-1 cells secrete more vesicles, which contain a similar amount of catecholamine to control cells. (**A**) Examples of amperometric spike activity recorded from control (upper) and Munc13-1 cells (lower trace). Bars represent 10 pA, 1 s. (**B**) A plot of the amperometric charge against the number of spikes for control (open circles) and Munc13-1 cells (closed circles) shows a similar, linear relation. The difference in the number of spikes is statistically significant (p <0.02; t-test). (**C**) The average charge per vesicle was also similar in control and Munc13-1 cells [1.72 ± 0.19 pC (n = 12) and 1.86 ± 0.33 pC (n = 10), respectively]. Error bars represent SEM.

increase in membrane capacitance was mediated by the fusion of catecholamine-containing vesicles (Figure 2A, bottom trace, red). Further analysis demonstrated that both the exocytotic burst (measured up to 1 s after the flash) and the sustained component (measured 1–5 s after the flash) were increased in Munc13-1 cells (Figure 2A and B; Table I). On average, the exocytotic burst increased from 476.2 ± 62.6 fF (n = 19) in control cells to 1484.6 ± 227.2 fF [n = 17; p <0.001 (t-test)] in cells overexpressing Munc13-1, while the sustained component increased from 173.1 ± 51.9 fF (n = 19) to 630.0 ± 143.7 fF [n = 17; p <0.001 (t-test)].

We have shown previously that Munc13-1 acts as a phorbol ester-dependent enhancer of transmitter release when overexpressed presynaptically in the *Xenopus* neuromuscular junction (Betz *et al*., 1998). In the present study, however, phorbol ester application on Munc13-1 cells before flash stimulation did not lead to a further increase in secretion (data not shown), although we observed translocation of the molecule to the plasma membrane. These data suggest that the amount of Munc13-1 located at the plasma membrane before phorbol

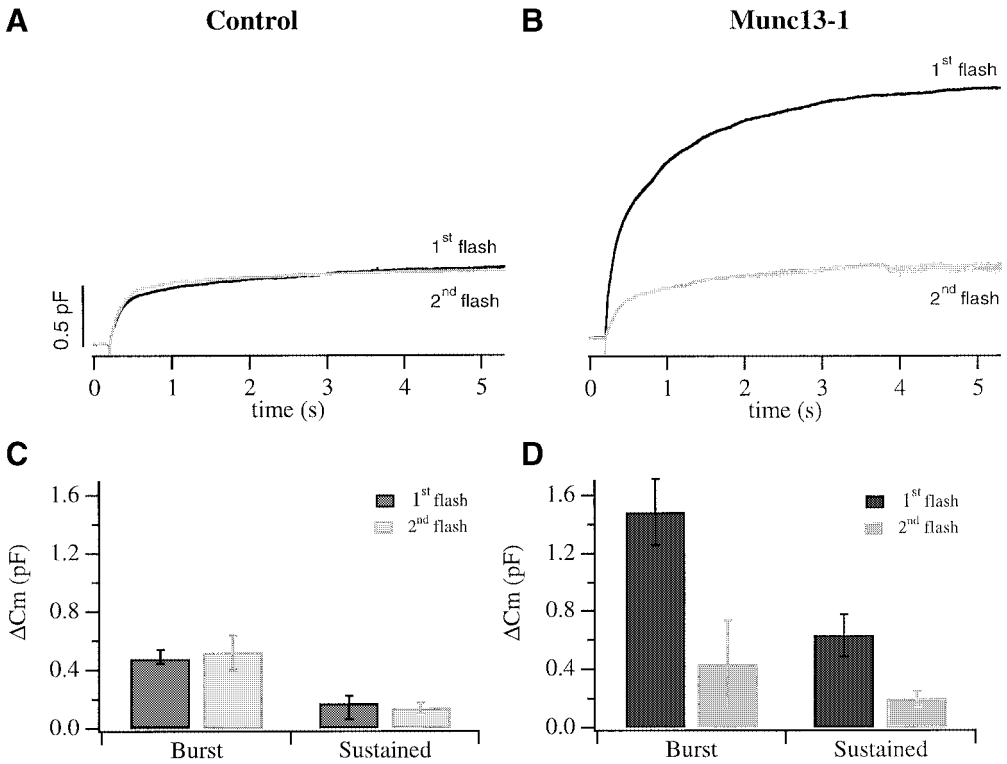

Fig. 5. Catecholamine secretion in response to a second flash is significantly smaller in Munc13-1 cells. (**A**) The average response to a second flash in control cells (gray) was similar to the response to the first flash (black). (**B**) In contrast, secretion in response to the second flash in Munc13-1 cells (gray) was three to four times smaller than the response to the first flash (black). The burst amplitude of the second flash response was reduced to 65% of the first flash response in Munc13-1 cells (**D**), while it was similar in control cells (**C**). The amplitudes of the sustained component of the second flash response were reduced to 65% and 45% of the first flash response in Munc13-1 (D) and control cells (C), respectively. Error bars represent SEM.

ester application (see Figure 1C, left) was already sufficient to mediate the observed increase in secretion. In order to elucidate further the contribution of the C1 domain, we overexpressed Munc13-1^{H567K}. This protein carries a point mutation in the Cys_6His_2 motif of the C1 domain and therefore no longer binds phorbol ester (Betz *et al*., 1998). As shown in Figure 2A (middle trace, blue), the exocytotic burst in Munc13-1^{H567K}-overexpressing cells was 942 ± 208 fF (n = 15), while the sustained component was 282 ± 74. fF (n = 14), both significantly greater than in control cells [p <0.001 (t-test)]. However, the increase in secretion was much less pronounced than with wild-type Munc13-1. Thus, we conclude that the C1 domain facilitates the action of Munc13-1, but is not an absolute requirement for Munc13-1 function. Chromaffin cells infected with GFP alone did not show a significant increase in any of the kinetic components of secretion [345.1 ± 81 fF (n = 5) for the exocytotic burst and 180.0 ± 79 fF (n = 5) for the sustained component], demonstrating that the observed increase in secretion was exclusively due to the presence of Munc13-1 or Munc13-1^{H567K}, respectively. In addition, we found that resting $[Ca^{2+}]_i$, which has been reported to increase secretion considerably (Neher and Zucker, 1993; von Rüden and Neher, 1993; Neher, 1998; Smith *et al*., 1998), was low in intact control (68.6 ± 7.3 nM; n = 20) and Munc13-1 cells (69.1 ± 7.4 nM; n = 25), ruling out that the enhanced secretion in Munc13-1 cells was due to a higher resting $[Ca^{2+}]_i$.

To investigate further the observed effect of Munc13-1, we analyzed the kinetics and amount of secretion during the exocytotic burst in more detail. In control cells, the exocytotic burst can be further resolved into two components. The fast burst component is mediated by the RRP, which contains vesicles that fuse with a time constant of ~30 ms upon Ca^{2+} elevation to 20 μM. The slow burst component is mediated by the SRP, which represents vesicles that fuse with a slower time constant of ~300 ms upon Ca^{2+} elevation to 20 μM (Voets *et al*., 1999). Munc13-1-overexpressing cells exhibited a 2- to 3-fold increase in the size of both fast [RRP; Figure 2C, left; Table I; p <0.02 (t-test)] and slow burst component (SRP; Figure 2C, right; Table I; p <0.02 (t-test)], suggesting the existence of more vesicles in both of these pools. However, no significant change in the SRP:RRP ratio was observed, suggesting that the equilibrium constant between these pools was not significantly altered. The time constants of secretion during the fast and the slow burst components in Munc13-1 cells were also comparable to those in control cells (Figure 2C; Table I). Furthermore, the dependencies of the time constants and of the threshold for fusion on $[Ca^{2+}]_i$ in Munc13-1 cells were not significantly different from those in control cells (data not shown). Thus, we conclude that the large increase in secretion is not due to a change in the Ca^{2+} dependence for fusion.

The number of 'morphologically docked' vesicles is unchanged in Munc13-1 cells

The observed increase in Munc13-1 cells might be due to an increase in the number of vesicles, which are located

near the plasma membrane ('morphologically docked'). To test this possibility, we performed electron microscopy experiments and compared the number of vesicles close to the plasma membrane in Munc13-1 cells to that in control cells. As shown for two representative cells in Figure 3, the overall morphology of Munc13-1-overexpressing cells was similar to that of control cells, demonstrating that the massive overexpression did not affect the distribution of granules within the cells. Quantitative analysis revealed that the number of vesicles located within 200 nm of the plasma membrane was similar in Munc13-1 and control cells (Figure 3C), ruling out the possibility that the increase in secretion in Munc13-1 cells was mediated by an increased number of 'morphologically docked' vesicles.

Enhanced secretion in Munc13-1 cells results from release of more vesicles

At least two other possibilities could account for the enhanced increase in membrane capacitance and the larger amperometric signal: (i) the fusion of more vesicles, which contain the same amount of catecholamine as those in control cells; (ii) the fusion of larger vesicles, which contain more catecholamine. To distinguish between these possibilities, we compared the number of amperometric spikes, which correspond to the fusion of single vesicles, with the integral of the amperometric current, which correlates with the amount of catecholamine secreted, i.e. charge (Schroeder *et al*., 1996). Since the amperometric spikes in flash experiments overlapped and were therefore difficult to separate, we used a more moderate stimulation for this analysis. Cells were depolarized with 60 mM KCl and the resulting amperometric spikes were counted and compared with the integral of the amperometric currents. Consistent with our finding in flash experiments, Munc13-1 cells showed greater amperometric activity (Figure 4A and B). The average number of spikes during a 30 s stimulation was 48.6 ± 8.2 (n = 12) in control and 106.9 ± 20.03 (n = 10) in Munc13-1 cells, respectively [p <0.02 (t-test)]. However, the relation between the number of vesicles detected and the integral of the amperometric currents was linear and indistinguishable from that for control cells (Figure 4B). The average charge per vesicle, measured from single amperometric spikes, was similar in both populations and comparable to previously published data (Figure 4C; Chow *et al*., 1992), ruling out a function for Munc13-1 as a regulator of catecholamine transport. Thus, this series of experiments, as well as the higher spike activity observed in flash experiments, demonstrated that the enhanced secretion in Munc13-1 cells occurs via fusion of more vesicles.

Munc13-1 causes depletion of available vesicles within a single flash stimulation

In control cells, secretion during the sustained component continued for at least 5 s at a constant rate, as long as $[Ca^{2+}]_i$ was kept constant (Figure 2; Xu *et al*., 1998). Although secretion during the sustained component was larger in Munc13-1 cells (Figure 2A and B; Table I), its rate decreased noticeably from 416 fF/s (1–1.5 s after the flash) to 30.2 fF/s (4.5–5 s after the flash). To examine whether the observed decrease was due to pool depletion we applied a second flash 2 min after the first flash. In general, RRP and SRP recovery after pool depletion

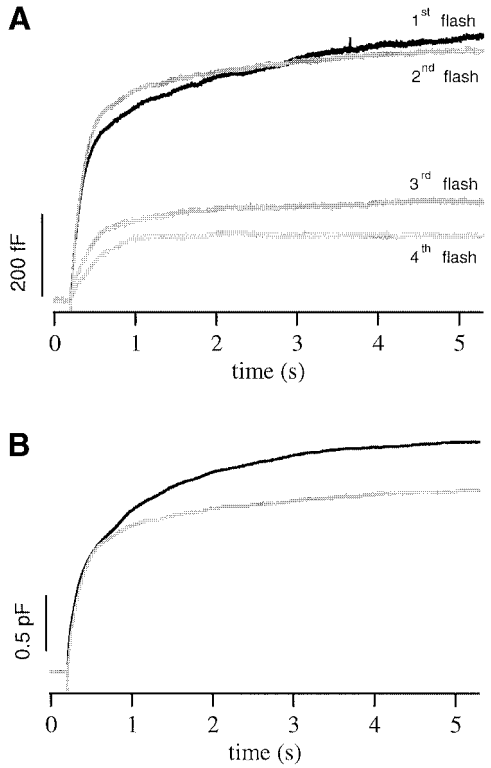

Fig. 6. Control cells contain a limited number of releasable vesicles. (**A**) Average membrane capacitance increase in control cells for four successive flashes given at 2 min intervals. The responses to the first two flashes were similar, but the third and fourth flashes led to significantly smaller responses. (**B**) The sum of the four flash responses from control cells (gray) was still smaller than the averaged response to the first flash in Munc13-1 cells (black).

occurs within 1 min (von Rüden and Neher, 1993; Smith *et al*., 1998). In control cells, the average exocytotic burst of the second flash was almost identical to the first flash while the sustained component was only slightly smaller (Figure 5A and C; Table I). In contrast, following the massive secretion during the first flash stimulation in Munc13-1 cells, the response to the second flash was significantly reduced (Figure 5B and D; Table I). The average exocytotic burst of the second flash was 70% smaller than the exocytotic burst during the first flash [430.0 ± 295.5 fF (n = 17) and 1484.6 ± 227.2 fF, (n = 17), respectively]. The sustained component of the second flash was 65% smaller than the sustained component during the first flash [202.2 ± 50.1 fF (n = 17) and 630.0 ± 143.7 fF (n = 17), respectively]. These data imply that, in Munc13-1 cells, depletion of available vesicles occurs during the first flash stimulation.

To investigate whether a control cell could secrete as many vesicles as Munc13-1 cells, we applied four successive flashes at 2 min intervals to control cells and measured the increase in capacitance after each flash. Under our experimental conditions, exocytosis occurred only during the stimulation intervals (5 s) and then ceased rapidly since $[Ca^{2+}]_i$ returned to its buffered value of 200–300 nM. As shown in Figures 5A and 6A, the responses to the first two flashes were similar. However, the third and the fourth flashes elicited significantly smaller responses (Figure 6A), and there was no response to a fifth flash (not shown). This can be explained by depletion of available vesicles and

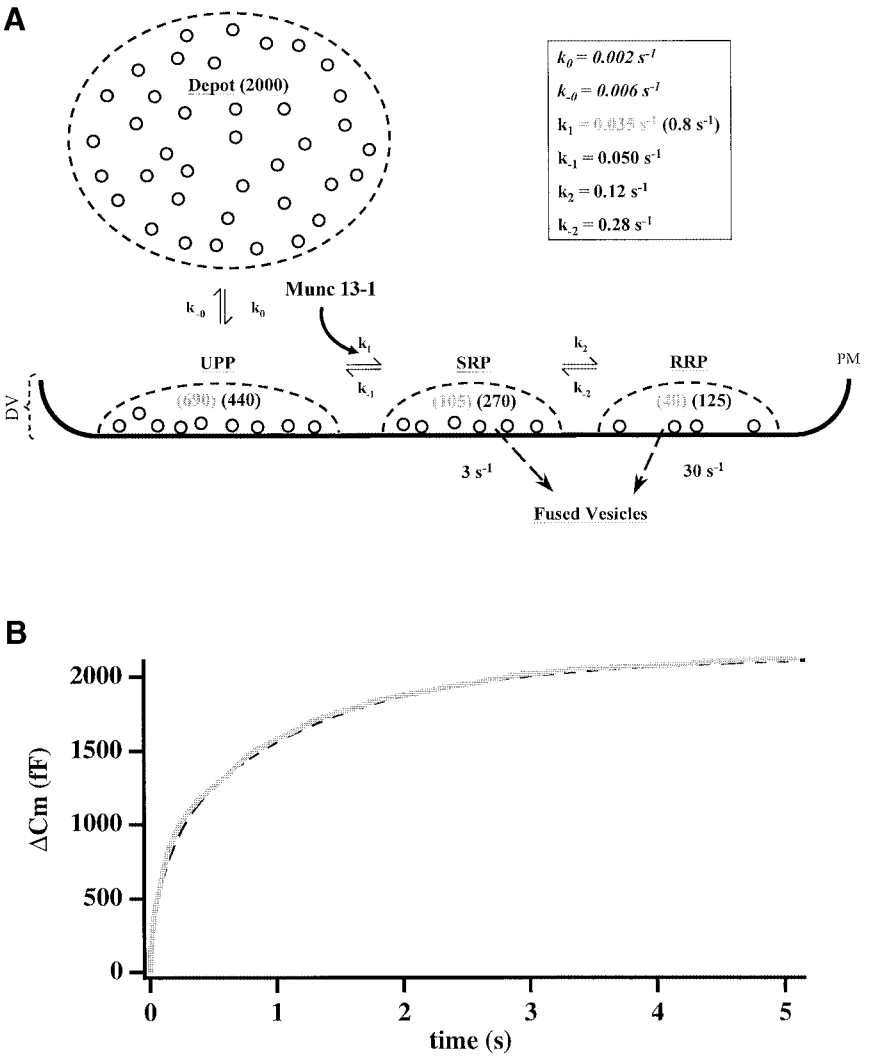

Fig. 7. A refined model for secretion in chromaffin cells. (**A**) According to this model, vesicles can reside in four separate states or pools. The estimated number of vesicles in each pool at steady state is indicated in brackets (gray for control; black for Munc13-1). The model predicts that Munc13-1 increases the forward rate constant (k_1) from the unprimed pool (UPP) to the SRP by a factor of 20–30. (**B**) Simulation of secretion for Munc13-1 cells (dashed line) according to the parameters given in (A) yields an excellent fit for the experimental data (gray line). PM, plasma membrane; DV, docked vesicles.

washout of intracellular factors that are needed for secretion (Augustine and Neher, 1992; Burgoyne, 1995). The sum of the responses to the four successive flashes in control cells (Figure 6B; gray) was only 22% smaller than the averaged response to the first flash in Munc13-1 cells (Figure 6B; black). Thus, as in Munc13-1 cells, secretion from control cells decreased significantly after exocytosis of a large number of vesicles following several, successive stimulations, suggesting that another, very slow step of vesicle supply becomes rate-limiting. These data also indicate that, under our experimental conditions, refilling does not derive from the large depot pool, which has been shown to be much larger than the sum of the four flash responses (Augustine and Neher, 1992).

Discussion

Overexpression of Munc13-1 increases secretion by priming LDCVs

In several secretory systems, the number of readily releasable vesicles is smaller than the number of docked vesicles (Parsons *et al*., 1995; Steyer *et al*., 1997; Oheim *et al*., 1998). This led to the proposal that docked vesicles have to undergo one or more maturation steps ('priming') before they become fusion-competent. In the present study we investigated whether Munc13-1 can act as a priming factor for LDCVs in chromaffin cells.

We demonstrate that Munc13-1 causes a 2- to 3-fold increase in the two components of the exocytotic burst (Figure 2). The enhanced secretion results from exocytosis of more vesicles, which contain similar amounts of catecholamine to those in control cells (Figure 4), without affecting the time constants for fusion. Munc13-1 accelerates vesicle maturation during the flash stimulation, which is reflected by enhanced secretion during the sustained component (Figure 2). We also observed that the rate of secretion had already decreased during the first flash stimulation and that secretion recovered only partially in the second flash, suggesting a depletion of available vesicles (Figures 5 and 6). Interestingly, the average amount of exocytosis in Munc13-1 cells during the first flash was 2100 fF, corresponding to ~840 vesicles

Table I. Effects of Munc13-1 on different secretion components

	Exocytotic burst		Sustained component	
	Control	Munc13-1	Control	Munc13-1
Amplitude (fF)				
first flash	476.2 ± 62.6 (n = 19)	1484.6 ± 227.2 (n = 17)[a]	173.1 ± 51.9 (n = 19)	630.0 ± 143.7 (n = 17)[a]
second flash	519.1 ± 117.6 (n = 19)	430.0 ± 295.5 (n = 17)	141.7 ± 37.2 (n = 19)	202.2 ± 50.1 (n = 17)
	Fast exocytotic burst		Slow exocytotic burst	
	Control	Munc13-1	Control	Munc13-1
First flash				
amplitude (fF)	100.3 ± 33.9 (n = 19)	265.7 ± 61.3 (n = 17)[b]	315.3 ± 40.6 (n = 19)	676.1 ± 132.3 (n = 17)[b]
time constant (ms)	37.8 ± 7.4 (n = 19)	31.5 ± 9.4 (n = 17)	177.9 ± 13.9 (n = 19)	167.9 ± 26.8 (n = 17)

Values represent mean ± SEM.
[a]p <0.001, [b]p <0.02 (t-test).

(assuming 2.5 fF/vesicle). This value agrees well with the number of 'morphologically docked' vesicles in bovine chromaffin cells (Figure 3; Parsons *et al*., 1995; Plattner *et al*., 1997; Steyer *et al*., 1997; Oheim *et al*., 1998), suggesting that all 'morphologically docked' vesicles in Munc13-1 cells can be primed and released within a matter of seconds. Based on our findings we propose that Munc13-1 acts as a priming factor for docked LDCVs and that this pool is depleted during a single stimulation.

A refined model for secretion in chromaffin cells

Electrophysiological measurements on endocrine cells led to the identification of distinct pools of vesicles that represent different stages of vesicle maturation along the secretory pathway [see Henkel and Almers (1996) and Neher (1998) for reviews]. A direct equilibrium between a large reserve pool (depot pool) and a releasable pool of vesicles was proposed in the initial two-step model by Heinemann *et al*. (1993). Voets *et al*. (1999) refined the model by seperating the main releasable pool of vesicles into two distinct pools, RRP and SRP, according to their fusion kinetics.

The physiological results obtained in the present study in conjunction with the morphological data suggest that the delivery of vesicles to the releasable pools (SRP and RRP) does not occur directly from the depot pool. Further support for this notion comes from the findings that refilling of RRP and SRP following pool depletion occurs within 10-60 s (von Rüden and Neher, 1993; Moser and Neher, 1997; Smith *et al*., 1998; Voets *et al*., 1999), while partial redocking of vesicles occurs with a much slower time constant of 6 min (Steyer *et al*., 1997; Steyer and Almers, 1999). We propose that another functional pool, which we define as the unprimed vesicle pool (UPP), exists between the depot pool and the releasable pools. Vesicles in the UPP are physically near the plasma membrane, but functionally, they have to undergo one or more steps of maturation before they become fusion-competent. Vesicles in RRP, SRP and UPP represent the population of 'morphologically docked' vesicles. A small fraction of the docked vesicles has already matured under resting conditions and represents the readily releasable pools of vesicles (SRP and RRP) that can be released within less than a second after elevation of $[Ca^{2+}]_i$.

A working model for LDCV docking, priming and fusion is illustrated in Figure 7A. In this model, vesicles can reside in any of four separate pools, representing different functional states or maturation steps. Vesicles from the depot pool translocate to the membrane to join the UPP with a forward rate constant k_0 and a backward rate constant k_{-0}. Vesicles in the UPP are primed into the SRP with a forward rate constant k_1. We assume that k_1 is the well-defined calcium-dependent step (Heinemann *et al*., 1993). Vesicles in the SRP can either return to the UPP, with a rate constant k_{-1}, or move to the RRP, with a rate constant k_2. Finally, vesicle fusion upon stimulation is represented by a transition to 'fused vesicles' and contributes to the increase of membrane capacitance. Vesicles in the SRP fuse with a typical rate constant of ~3–6 s^{-1}, while vesicles in the RRP fuse with a typical rate constant of ~20–50 s^{-1} (Voets *et al*., 1999).

Munc13-1 accelerates priming of docked vesicles

We have solved numerically the matrix describing this model (see Materials and methods) and found that changing any rate constant except k_1 does not explain our results and gives a poor fitting to the experimental data. For example, if we assume that Munc13-1 enhances the docking of more vesicles (by accelerating k_0), we would expect an increase in both burst components and the sustained component as well as a large response during the second flash. We observed a decrease in response to the second flash (Figure 5) and so consider this possibility unlikely. Our finding that the number of 'morphologically docked' vesicles in chromaffin cells overexpressing Munc13-1 is similar to that in control cells (Figure 3) also argues strongly against a role of Munc13-1 in LDCV docking. If, on the other hand, Munc13-1 were to change k_2/k_{-2}, we would expect a difference in the ratio between RRP and SRP. Our data clearly demonstrate that SRP and

RRP increase by a similar factor in Munc13-1 cells, thus ruling out an effect of Munc13-1 on k_2/k_{-2}.

We can explain all the effects reported in this study only if we assume that Munc13-1 changes the equilibrium between UPP and SRP by accelerating k_1. Under steady-state conditions in Munc13-1 cells, increasing k_1 increases the number of vesicles in the SRP and subsequently also in the RRP, while the number of vesicles in the UPP will decrease (Figure 7A). This is why we found enhanced exocytosis in both components of the exocytotic burst during stimulation. The sustained component is also increased, but its decreased rate towards the end of the flash stimulation indicates a depletion of release-competent vesicles. This depletion occurs because, upon stimulation, the remaining vesicles in the UPP are transferred to the SRP at a high rate (k_1) and will subsequently fuse. Following the first stimulation, k_0 becomes the rate-limiting step (Steyer *et al*., 1997) and we measure only a small response in the second flash (Figure 5A; Table I). Thus, our data imply that Munc13-1 acts as a priming factor for morphologically docked, but unprimed vesicles. However, it is unlikely that Munc13-1 is the sole priming factor for large dense-core vesicles. Munc13-1 is almost undetectable in chromaffin cells from newborn mice (our unpublished data) and is expressed at very low levels in adult adrenal chromaffin cells (Figure 1). More importantly, measurements from adrenal slices of Munc13-1 knockout mice revealed no noticeable difference in the amount and kinetics of secretion when compared with control cells (our unpublished data), suggesting the presence of additional priming factors. By computer simulation, we estimate that Munc13-1 increases k_1 by a factor of 20–30. As shown in Figure 7B, simulation of secretion from Munc13-1 cells according to the above parameters yields an excellent fit for our experimental data.

Although Munc13-1 has the most dramatic effect on the number of release-competent vesicles reported so far, others factors might also modulate the size of the release-competent vesicle pools. Protein kinase C (PKC), for example, increases both RRP and SRP size in bovine chromaffin cells by a factor of at least 2 (Gillis *et al*., 1996). Furthermore, the reported temperature-dependent step, which occurs after docking (Bittner and Holz, 1992), probably correlates with our proposed priming step. Finally, the pH of the secretory cell, which affects the size of release-competent pools (Thomas *et al*., 1993b), might also affect the rate constant k_1. However, it should be noted that these factors only have a modulatory role on the priming reaction, while the data from Munc13-1 knockout mice indicate that Munc13-1 is, at least in most neurons, an essential requirement for priming (Aravamudan *et al*., 1999; Augustin *et al*., 1999b; Richmond *et al*., 1999).

A putative molecular mechanism for Munc13-1 action

Recently, it was shown that a SNAP-25-specific antibody inhibits the fast component of the exocytotic burst. It was suggested that the SRP contains vesicles that form loose SNARE complexes, while the RRP contains vesicles that form tight SNARE complexes (Xu *et al*., 1999b). The step acted on by Munc13-1 coincides with the formation of the loose core complex. The availability of syntaxin, a key component of the SNARE complex, is probably down-regulated by its interaction with Munc18 (Misura *et al*., 2000). Recently, it was shown that Munc13-1 can displace Munc18 from the syntaxin–Munc18 complex, thereby freeing syntaxin from Munc18-mediated negative regulation (Sassa *et al*., 1999). Since Munc13-1 also binds syntaxin in its open conformation (N.Brose and D.Fasshauer, unpublished observations), it might serve to release syntaxin from Munc18. We found that Munc18 is expressed in chromaffin cells and that Munc13-1 is expressed at very low levels under control conditions (Figure 1A). Thus, overexpression of Munc13-1 could accelerate the release of syntaxin from Munc18-mediated negative regulation and thereby lead to an increase in exocytosis.

Several studies suggest that, in addition to its priming action, Munc13-1 enhances transmission in a phorbol ester-dependent manner through its C1 domain (Betz *et al*., 1998; Lackner *et al*., 1999; Nurrish *et al*., 1999). It has also been shown that application of phorbol ester enhances the interaction with Doc2 and that inhibition of this interaction leads to a reduction of exocytosis in PC-12 cells (Orita *et al*., 1996) and cultured neurons (Mochida *et al*., 1998; but see also Hori *et al*., 1999). These data argue for an additional, modulatory role of Munc13-1 on regulated exocytosis. The presence of three C2-regulatory domains led to the suggestion that Munc13-1 might also act by binding calcium or phospholipids, thereby acting as an exocytotic Ca^{2+} sensor (Aravamudan *et al*., 1999). However, the dependency of the rate constants of secretion on $[Ca^{2+}]_i$ is not altered in Munc13-1-overexpressing cells, suggesting that Munc13-1 does not act as an exocytic calcium sensor (our unpublished data). Finally, its interaction with the cytoskeleton through spectrin (Sakaguchi *et al*., 1998) might also contribute to Munc13-1 action by rearranging the submembrane cytoskeleton. Further experiments to address the contribution of the different sites and domains are needed in order to elucidate the exact mechanism of Munc13-1 function.

Materials and methods

Chromaffin cell preparation and infection

Isolated bovine adrenal chromaffin cells and virus containing Munc13-1–GFP were prepared as described previously (Ashery *et al*., 1999). Infection was performed on cultured cells 5–48 h after plating or on freshly prepared cells. Initial detection was performed using an IX70 Olympus microscope with a filter set for enhanced GFP (excitation: HQ 470/40; dichroic: Q 495 LP; emission: HQ 525/50; AHF Analysentechnik, Tübingen, Germany).

Sodium dodecyl sulfate–polyacrylamide gel electrophoresis (SDS–PAGE) and western blotting experiments were performed according to standard procedures (Towbin *et al*., 1979). Antibodies to Munc13 isoforms (Augustin *et al*., 1999a) and to Munc18 (Hata *et al*., 1993) have been described previously.

Whole-cell patch–clamp and membrane capacitance measurements

Conventional whole-cell recordings and capacitance measurements were performed as detailed in Ashery *et al*. (1999) and analyzed in IGOR Pro (WaveMetrics Inc., Lake Oswego, OR). The external bathing solution contained 140 mM NaCl, 2.8 mM KCl, 2 mM $CaCl_2$, 1 mM $MgCl_2$, 10 mM HEPES and 2 mg/ml glucose (pH 7.2, 310–320 mOsm). For flash photolysis experiments the internal solutions consisted of (in mM): 105 cesium glutamate, 2 MgATP, 0.3 GTP, 33 HEPES, 0.33 Mg^{2+}–Fura-2, adjusted to pH 7.2 using HCl or CsOH (300–310 mOsm). The basal

$[Ca^{2+}]_i$ was buffered by a combination of 4 mM $CaCl_2$ and 5 mM NPE to give a free $[Ca^{2+}]_i$ of 200–300 nM (Xu *et al*., 1999a). Experiments were performed 18–36 h after infection at 30–32°C. Munc13-1–GFP-overexpressing cells were identified with an inverted Axiovert 10 microscope [excitation: 480 nm; dichroic: 505 LP; emission: 510 LP (AHF Analysentechnik)]. For kinetic analysis of secretion we fitted the capacitance traces with a triple exponential macro. The first two exponential components represent the fast and the slow burst components while the third exponential component corresponds to the sustained component. Values represent mean ± SEM

Photolysis of caged Ca^{2+} and $[Ca^{2+}]_i$ measurements

Flashes of UV light were generated by a flash lamp (Rapp Optoelektronik, Hamburg, Germany) and fluorescence excitation light was generated by a monochromator (TILL Photonics, Planegg, Germany) as described by Xu *et al*. (1997). The monochromator and flash lamp were coupled into the epifluorescence port of an inverted Axiovert 10 microscope equipped with a 100× Fluar objective (Zeiss, Oberkochem, Germany). Mg^{2+}–Fura-2 was excited at 340/380 nm with filter sets composed of dichroic: 400 LP, emission: HQ 510/40 (AHF Analysentechnik). The illumination area was reduced to a spot of ~15 µm diameter and the fluorescence detection area was adjusted using a view finder system (TILL Photonics) to cover only the diameter of the cell. Emission light was attenuated with a neutral density filter (OD 1.3; Coherent, Auburn, CA), detected with an avalanche photodiode (SPCM-AQ 231, EG&G Optoelectronics, Canada), filtered at 2 kHz and acquired with Pulse software (HEKA Elektronik, Lambrecht, Germany). Fluorescence excitation light was used to measure $[Ca^{2+}]_i$ and simultaneously photorelease Ca^{2+} after the flashes in order to keep $[Ca^{2+}]_i$ approximately constant. $[Ca^{2+}]_i$ was calculated from the fluorescence ratio R according to Grynkiewiez *et al*. (1985) and the flash photolysis efficiency was calculated as described before (Xu *et al*., 1998).

Amperometry

Carbon fiber electrodes were prepared as described previously (Schulte and Chow, 1996). A constant voltage of 780 mV versus an Ag/AgCl reference was applied to the electrode. The tip of the carbon fiber electrode was gently pressed against the cell surface. The amperometric current was recorded using an EPC-7 patch clamp amplifier (HEKA Electronik). Signals were sampled at 10 kHz and filtered at 2.9 kHz. Single amperometric events were detected with an IGOR macro adapted from Volker Scheuss counting the number of amperometric spikes above a threshold of 2.5 pA. This was compared in Figure 4 with the integral of the amperometric current derived from the same trace.

Model simulation

The transition of vesicles between the five different pools (Figure 7) was described in matrix notation by:

$$\frac{dP}{dt} = \begin{pmatrix} -k_0 & k_{-0} & 0 & 0 & 0 \\ k_0 & -(k_0+k_1) & k_{-1} & 0 & 0 \\ 0 & k_1 & -(k_{-1}+k_2+f_1) & k_{-2} & 0 \\ 0 & 0 & k_2 & -(k_{-2}+f_2) & 0 \\ 0 & 0 & f_1 & f_2 & 0 \end{pmatrix} \times P$$

where f_1 and f_2 are fusion rate constants, k_0, k_{-0}, k_1, k_{-1}, k_2 and k_{-2} are rate constants and P is the vector (depot UPP SRP RRP fused-vesicles)^T, with the compenents being the sizes of the respective pools. The above matrix was numerically solved using a fourth order Runge–Kutta integration scheme with Cash–Karp parameters for adjustment of step size. Simulations were performed in IGOR Pro (WaveMetrix Inc.). The estimated numbers of vesicles occupying the pools at steady state were derived from our analysis and calculated assuming 2.5 fF/vesicle (Neher and Marty, 1982; Chow *et al*., 1996). The value for the depot pool (5 pF, corresponding to 2000 vesicles) was adapted from Augustine and Neher (1992). Values for k_0 and k_{-0} were taken from evanescent-field fluorescence microscopy measurements assuming that the visible pool of vesicles in these studies represents those vesicles underneath the membrane which we define as UPP, SRP and RRP (Steyer *et al*., 1997; Oheim *et al*., 1999; Steyer and Almers, 1999). It should be noted that the k_0 value was calculated after stimulation and thus might be even smaller under control conditions. Other rate constants were taken from Voets *et al*. (1999) and Heinemann *et al*. (1994) and slightly changed according to the size of the pools measured in the present study. The initial pool sizes and rate constants used for the simulations are indicated in Figure 7A. Under steady state conditions, Munc13-1 causes only a 2- to 3-fold increase in the number of vesicles in SRP and RRP. However, during stimulation we estimate that Munc13-1 accelerates k_1 by a factor of 20–30. This might either indicate that other factors limit the number of releasable vesicles under steady-state conditions or that Munc13-1 function is accelerated upon stimulation.

Confocal and electron microscopy

Fluorescent images were taken with a confocal laser-scanning system consisting of an SLM 410 Zeiss confocal microscope with a 40× oil objective (n.a. 1.3). The displayed images represent a single cross-section through the center of the cell. PMA (Sigma, Steinheim, Germany) was added to the bath to obtain a final concentration of 100 nM. The f_R was calculated for each cell independently, eliminating differences arising from different Munc13-1–GFP expression levels.

For electron microscopy, chromaffin cells were plated on collagen-coated (32 µg/ml; Sigma) coverslips (Cellocate, Eppendorf, Germany) and infected with Munc13-1–GFP. 12–18 h after infection, cells were observed under a fluorescence microscope and the location of infected/control cells was mapped. Coverslips were then fixed [with 1.5 or 2.5% glutaraldehyde in 0.1 M phosphate buffer (PB; pH 7.4)] at room temperature, incubated on ice for 1 h and washed repeatedly with 0.1 M PB. Cells were post-fixed with 1% OsO_4 for 1 h on ice in the dark, washed and stained with 1% uranyl acetate for 40 min. Following dehydration through a series of ethanol solutions and propylene oxide, cells were incubated in a 1:1 mixture of propylene oxide and Epon resin for 1 h at room temperature. Cells were then embedded in Epon and polymerized for 48 h at 60°C. 70 nm ultrathin sections were collected on single-slot, pioloform-coated grids, post-stained (1% uranyl acetate for 20 min; lead citrate for 2 min) and observed under an EM109 Zeiss electron microscope. Pictures were taken with a 70 mm camera. 34 000× magnification was used to measure the distances from the plasma membrane to the granule center (Plattner *et al*., 1997). Measurements were done ⩽1300 nm from the plasma membrane. Distances histograms were created for each cell and the relative frequency of vesicles was calculated according to the number of vesicles counted in this area. Averaged histograms for control (n = 11) and Munc13-1 (n = 11) cells are displayed in Figure 3.

Acknowledgements

We thank Dr Christian Rosenmund for stimulating discussions and Drs Helmut Plattner and Elena Lukyanetz for advice on electron microscopy on chromaffin cells. We also thank Frauke Friedlein, Anke Bührmann and Sally Wenger for expert technical assistance. This work was supported by grants from the Deutsche Forschungsgemeinschaft (SFB 406/A1 to N.B., SFB 523/B4 to E.N. and Re 1092/3-2 to J.R.), and a Feodor Lynen–Minerva Fellowship (to U.A.). T.V. is a post-doctoral fellow of the Flemish Fund for Scientific Research. N.B. is a Heisenberg fellow of the Deutsche Forschungsgemeinschaft.

References

Aravamudan,B., Fergestad,T., Davis,W.S., Rodesch,C.K. and Broadie,K. (1999) *Drosophila* Unc-13 is essential for synaptic transmission. *Nature Neurosci.*, **2**, 965–971.

Ashery,U., Betz,A., Xu,T., Brose,N. and Rettig,J. (1999) An efficient method for infection of adrenal chromaffin cells using the Semliki Forest virus gene expression system. *Eur. J. Cell Biol.*, **78**, 525–532.

Augustin,I., Betz,A., Herrmann,C., Jo,T. and Brose,N. (1999a) Differential expression of two novel Munc13 proteins in rat brain. *Biochem. J.*, **337**, 363–371.

Augustin,I., Rosenmund,C., Südhof,T.C. and Brose,N. (1999b) Munc13-1 is essential for fusion competence of glutamatergic synaptic vesicles. *Nature*, **400**, 457–461.

Augustine,G.J. and Neher,E. (1992) Calcium requirements for secretion in bovine chromaffin cells. *J. Physiol.*, **450**, 247–271.

Betz,A., Ashery,U., Rickmann,M., Augustin,I., Neher,E., Südhof,T.C., Rettig,J. and Brose,N. (1998) Munc13-1 is a presynaptic phorbol ester receptor that enhances neurotransmitter release. *Neuron*, **21**, 123–136.

Bittner,M.A. and Holz,R.W. (1992) A temperature-sensitive step in exocytosis. *J. Biol. Chem.*, **267**, 16226–16229.

Burgoyne,R.D. (1991) Control of exocytosis in adrenal chromaffin cells. *Biochim. Biophys. Acta*, **1071**, 174–202.

Burgoyne,R.D. (1995) Fast exocytosis and endocytosis triggered by

depolarisation in single adrenal chromaffin cells before rapid Ca^{2+} current run-down. *Pflügers Arch.*, **430**, 213–219.

Chow,R.H., von Rüden,L. and Neher,E. (1992) Delay in vesicle fusion revealed by electrochemical monitoring of single secretory events in adrenal chromaffin cells. *Nature*, **356**, 60–63.

Chow,R.H., Klingauf,J., Heinemann,C., Zucker,R.S. and Neher,E. (1996) Mechanisms determining the time course of secretion in neuroendocrine cells. *Neuron*, **16**, 369–376.

Duncan,R.R., Don-Wauchope,A.C., Tapechum,S., Shipston,M.J., Chow,R.H. and Estibeiro,P. (1999) High-efficiency semliki forest virus-mediated transduction in bovine adrenal chromaffin cells. *Biochem. J.*, **342**, 497–501.

Ellis-Davies,G.C.R. and Kaplan,J.H. (1994) Nitrophenyl-EGTA, a photolabile chelator that selectively binds Ca^{2+} with high affinity and releases it rapidly upon photolysis. *Proc. Natl Acad. Sci. USA*, **91**, 187–191.

Gillis,K.D. (1995) Techniques for membrane capacitance measurements. In Sakmann,B. and Neher,E. (eds), *Single-Channel Recording*, 2nd edn. Plenum Press, New York, pp. 155–198.

Gillis,K.D., Mößner,R. and Neher,E. (1996) Protein kinase C enhances exocytosis from chromaffin cells by increasing the size of the readily releasable pool of secretory granules. *Neuron*, **16**, 1209–1220.

Grynkiewicz,G., Poenie,M. and Tsien,R.Y. (1985) A new generation of Ca^{2+} indicators with greatly improved fluorescence properties. *J. Biol. Chem.*, **260**, 3440–3450.

Hata,Y., Slaughter,C.A. and Südhof,T.C. (1993) Synaptic vesicle fusion complex contains *unc-18* homologue bound to syntaxin. *Nature*, **366**, 347–351.

Heinemann,C., von Rüden,L., Chow,R.H. and Neher,E. (1993) A two-step model of secretion control in neuroendocrine cells. *Pflügers Arch.*, **424**, 105–112.

Heinemann,C., Chow,R.H., Neher,E. and Zucker,R.S. (1994) Kinetics of the secretory response in bovine chromaffin cells following flash photolysis of caged Ca^{2+}. *Biophys. J.*, **67**, 2546–2557.

Henkel,A.W. and Almers,W. (1996) Fast steps in exocytosis and endocytosis studied by capacitance measurements in endocrine cells. *Curr. Opin. Neurobiol.*, **6**, 350–357.

Holz,R., Bittner,M.A., Peppers,S., Senter,R. and Eberhard,D. (1989) MgATP-independent and MgATP-dependent exocytosis. Evidence that MgATP primes adrenal chromaffin cells to undergo exocytosis. *J. Biol. Chem.*, **264**, 5412–5419.

Hori,T., Takai,Y. and Takahashi,T. (1999) Presynaptic mechanism for phorbol ester-induced synaptic potentiation. *J. Neurosci.*, **19**, 7262–7267.

Lackner,M.R., Nurrish,S. and Kaplan,J.M. (1999) Facilitation of synaptic transmission by EGL-30 $G\alpha_o$ and EGL-8PLCβ: DAG binding to unc-13 is required to stimulate acetylcholine release. *Neuron*, **24**, 335–346.

Liljeström,P. and Garoff,H. (1991) A new generation of animal cell expression vectors based on the Semliki Forest virus replicon. *Biotechnology*, **9**, 1356–1361.

Misura,K.M.S., Scheller,R.H. and Weis,W.I. (2000) Three-dimensional structure of the neuronal–Sec1–syntaxin 1a complex. *Nature*, **404**, 355–362.

Mochida,S., Orita,S., Sakaguchi,G., Sasaki,T. and Takai,Y. (1998) Role of the Doc2a–Munc13-1 interaction in the neurotransmitter release process. *Proc. Natl Acad. Sci. USA*, **95**, 11418–11422.

Morgan,A. and Burgoyne,R.D. (1997) Common mechanisms for regulated exocytosis in the chromaffin cell and the synapse. *Seminars Cell Dev. Biol.*, **8**, 141–149.

Moser,T. and Neher,E. (1997) Rapid exocytosis in single chromaffin cells recorded from mouse adrenal slices. *J. Neurosci.*, **17**, 2314–2323.

Neher,E. (1998) Vesicle pools and Ca^{2+} microdomains: new tools for understanding their roles in neurotransmitter release. *Neuron*, **20**, 389–399.

Neher,E. and Marty,A. (1982) Discrete changes in cell membrane capacitance observed under conditions of enhanced secretion in bovine adrenal chromaffin cells. *Proc. Natl Acad. Sci. USA*, **79**, 6712–6716.

Neher,E. and Zucker,R.S. (1993) Multiple calcium-dependent processes related to secretion in bovine chromaffin cells. *Neuron*, **10**, 21–30.

Nurrish,S., Ségalat,L. and Kaplan,J.M. (1999) Serotonin inhibition of synaptic transmission: $G\alpha_o$ decreases the abundance of UNC-13 at release sites. *Neuron*, **24**, 231–242.

Oheim,M., Loerke,D., Stühmer,W. and Chow,R.H. (1998) The last few milliseconds in the life of a secretory granule. Docking, dynamics and fusion visualized by total internal reflection fluorescence microscopy (TIRFM). *Eur. Biophys. J.*, **27**, 83–98.

Oheim,M., Loerke,D., Stühmer,W. and Chow,R.H. (1999) Multiple stimulation-dependent processes regulate the size of the releasable pool of vesicles. *Eur. Biophys. J.*, **28**, 91–101.

Orita,S., Sasaki,T., Komuro,R., Sakaguchi,G., Maeda,M., Igarashi,H. and Takai,Y. (1996) Doc2 enhances Ca^{2+}-dependent exocytosis from PC12 cells. *J. Biol. Chem.*, **271**, 7257–7260.

Parsons,T.D., Coorssen,J.R., Horstmann,H. and Almers,W. (1995) Docked granules, the exocytic burst, and the need for ATP hydrolysis in endocrine cells. *Neuron*, **15**, 1085–1096.

Plattner,H., Artalejo,A.R. and Neher, E. (1997) Ultrastructural organization of bovine chromaffin cell cortex—analysis by cryofixation and morphometry of aspects pertinent to exocytosis. *J. Cell Biol.*, **139**, 1709–1717.

Richmond,J.E., Davis,W.S. and Jorgensen,E.M. (1999) UNC-13 is required for synaptic vesicle fusion in *C. elegans*. *Nature Neurosci.*, **2**, 959–964.

Sakaguchi,G., Orita,S., Naito,A., Maeda,M., Igarashi,H., Sasaki,T. and Takai,Y. (1998) A novel brain-specific isoform of β spectrin: isolation and its interaction with Munc13. *Biochem. Biophys. Res. Commun.*, **248**, 846–851.

Sassa,T., Harada,S., Ogawa,H., Rand,J.B., Maruyama,I.N. and Hosono,R. (1999) Regulation of the UNC-18–*Caenorhabditis elegans* syntaxin complex by UNC-13. *J. Neurosci.*, **19**, 4772–4777.

Schroeder,T.J., Borges,R., Finnegan,J.M., Pihel,K., Amatore,C. and Wightman,R.M. (1996) Temporally resolved, independent stages of individual exocytotic secretion events. *Biophys. J.*, **70**, 1061–1068.

Schulte,A. and Chow,R.H. (1996) A simple method for insulating carbon-fiber microelectrodes using anodic electrophoretic deposition of paint. *Anal. Chem.*, **68**, 3054–3058.

Smith,C., Moser,T., Xu,T. and Neher,E. (1998) Cytosolic Ca^{2+} acts by two separate pathways to modulate the supply of release-competent vesicles in chromaffin cells. *Neuron*, **20**, 1243–1253.

Steyer,J.A., Horstmann,H. and Almers,W. (1997) Transport, docking and exocytosis of single secretory granules in live chromaffin cells. *Nature*, **388**, 474–478.

Steyer,J.A. and Almers,W. (1999) Tracking single secretory granules in live chromaffin cells by evanescent-field fluorescence microscopy. *Biophys. J.*, **76**, 2262–2271.

Südhof,T.C. (1995) The synaptic vesicle cycle: a cascade of protein–protein interactions. *Nature*, **375**, 645–653.

Thomas,P., Wong,J.G. and Almers,W. (1993a) Millisecond studies of secretion in single rat pituitary cells stimulated by flash photolysis of caged Ca^{2+}. *EMBO J.*, **12**, 303–306.

Thomas,P., Wong,J.G., Lee,A.K. and Almers,W. (1993b) A low affinity Ca^{2+} receptor controls the final step in peptide secretion from pituitary melanotrophs. *Neuron*, **11**, 93–104.

Towbin,H., Staehelin,T. and Gordon,J. (1979) Electrophoretic transfer of proteins from polyacrylamide gels to nitrocellulose sheets: procedure and some applications. *Proc. Natl Acad. Sci. USA*, **76**, 4350–4354.

Voets,T., Neher,E. and Moser,T. (1999) Mechanisms underlying phasic and sustained secretion in chromaffin cells from mouse adrenal slices. *Neuron*, **23**, 607–615.

von Rüden,L. and Neher,E. (1993) A Ca-dependent early step in the release of catecholamines from adrenal chromaffin cells. *Science*, **262**, 1061–1065.

Xu,T., Naraghi,M., Kang,H. and Neher,E. (1997) Kinetic studies of Ca^{2+} binding and Ca^{2+} clearance in the cytosol of adrenal chromaffin cells. *Biophys. J.*, **73**, 532–545.

Xu,T., Binz,T., Niemann,H. and Neher,E. (1998) Multiple kinetic components of exocytosis distinguished by neurotoxin sensitivity. *Nature Neurosci.*, **1**, 192–200.

Xu,T., Ashery,U., Burgoyne,R.D.,and Neher,E. (1999a) Early requirement for α-SNAP and NSF in the secretory cascade in chromaffin cells. *EMBO J.*, **18**, 3293–3304.

Xu,T., Rammner,B., Margittai,M., Artalejo,A.R., Neher,E. and Jahn,R. (1999b) Inhibition of SNARE complex assembly differentially affects kinetic components of exocytosis. *Cell*, **99**, 713–722.

Received February 23, 2000; revised May 17, 2000; accepted May 19, 2000